Medicine in Novel Technology and Devices 9 (2021) 100050

Contents lists available at ScienceDirect

Medicine in Novel Technology and Devices

journal homepage: www.journals.elsevier.com/medicine-in-novel-technology-and-devices/

Research Paper

Computational models of flatfoot with three-dimensional fascia and bulk soft tissue interaction for orthosis design

Yinghu Peng [a,b], Duo Wai-Chi Wong [a,b], Yan Wang [a,b], Tony Lin-Wei Chen [b], Guoxin Zhang [b], Fei Yan [b], Ming Zhang [a,b,*]

[a] The Hong Kong Polytechnic University Shenzhen Research Institute, Shenzhen, China
[b] Department of Biomedical Engineering, Faculty of Engineering, The Hong Kong Polytechnic University, Hong Kong, China

ARTICLE INFO

Keywords:
Plantar fascia
Foot-ankle complex
Flatfoot
Biomechanics
Finite element analysis

ABSTRACT

The finite element (FE) method has been widely used to investigate the internal force of plantar fascia, which could reveal the relationship between plantar fascia dysfunction and flatfoot deformity during weight-bearing conditions. However, for most foot FE models, plantar fascia utilized truss elements or three-dimensional geometry that did not consider the interaction between plantar fascia and bulk soft tissue. These configurations could ignore the impact of superoinferior loading induced by arch support and underestimate the plantar fascia loading. This study aims to investigate how the fascia-bulk soft tissue interaction affects the internal foot biomechanics in the flatfoot FE analysis with a three-dimensional plantar fascia model, which included both fascia-bone and fascia-bulk soft tissue interactions (3DBPT). To evaluate the effect of fascia-bulk soft tissue interaction on internal foot mechanics, this study compared the 3DBPT model with the other two plantar fascia models, including linear fascia (BPL) and three-dimensional plantar fascia without fascia-bulk soft tissue interaction (3DBP). The predicted foot contact pressure in the 3DBPT model was compared with the measured value obtained by the F-Scan pressure measurement system in balanced standing. Peak von Mises stresses in the plantar fascia and foot ligaments were reported. The stress of the plantar fascia in the 3DBPT model was higher than that of 3DBP. In the 3DBPT model, the superoinferior loading exerted on the bulk soft tissue could be directly transferred to the plantar fascia. The proposed model, including the plantar fascia and bulk soft tissue interaction, could reveal relatively reliable plantar fascia loading in flatfoot deformity, thereby contributing to the development of orthotic designs for the flatfoot deformity.

1. Introduction

The plantar fascia is the primary passive plantar tissue that supports the medial longitudinal arch, which can absorb the impact of ground reaction force in running or jumping [1–4]. During weight-bearing conditions, the loading applied to the foot tightened the plantar fascia, forming a tie-rod of the medial longitudinal arch. The dysfunction of plantar fascia could affect the height and shape of the medial longitudinal arch [2,4,5]. Previous studies have reported that plantar fascia morphology and dysfunction are related to flatfoot deformity [2,4,5]. To investigate the biomechanical response of plantar fascia to loading, efficient and effective computational tools, such as the finite element (FE) method, have been developed [6–8]. For the FE approach, a reliable model is essential to assess the stress distribution of the plantar fascia in flatfoot deformity because the accuracy of the model could affect our understanding of the mechanical role of fascia in foot posture.

Previous studies have developed numerous foot FE models, which adopted multiple configurations for the plantar fascia to investigate its mechanical roles in foot posture [9–13]. In most foot FE models, the plantar fascia structure was typically simplified as truss elements, connecting the heel and each foot ray [9,11,13–15]. However, the distribution of fascia stress and strain could not be demonstrated in linear elements. One-dimensional ligaments could even distort the model, thereby affecting the biomechanics in the plantar fascia [16]. To better imitate the function of fascia, some studies have established more detailed three-dimensional plantar fascia geometries in the foot models

* Corresponding author. Department of Biomedical Engineering, Faculty of Engineering, The Hong Kong Polytechnic University, Hung Hom, Kowloon, Hong Kong, China.
E-mail address: ming.zhang@polyu.edu.hk (M. Zhang).

[1] 3DBPT: three-dimensional plantar fascia model with both fascia-bone and fascia-bulk soft tissue interactions.

https://doi.org/10.1016/j.mednotd.2020.100050
Received 24 August 2020; Received in revised form 8 October 2020; Accepted 27 October 2020

[3,9,16,17]. Although these models adopted three-dimensional plantar fascia and considered the connection between plantar fascia and bones, the interaction between bulk soft tissue and plantar fascia was not included. Compared with the normal foot, the foot-ground contact area of flatfoot increased, especially in the midfoot region during balanced standing [18]. Without fascia-bulk soft tissue interaction, the force exerted on the interface between the ground and sole cannot be directly transmitted to the plantar fascia through the bulk soft tissue in the model [17], which may affect the stress distributions of the fascia. Simplified plantar fascia modelling or configurations could even affect our understanding of the relationship between plantar fascia dysfunction and flatfoot deformity. Therefore, developing a more detailed foot-ankle complex model that included the plantar fascia and bulk soft tissue interaction is of great significance for indicating the deterioration of plantar fascia, thereby contributing to the optimization of the orthotic insole in the flatfoot deformity.

This study aims to investigate how the fascia-bulk soft tissue interaction affects the internal foot biomechanics in the flatfoot FE analysis with a three-dimensional plantar fascia model, which included both fascia-bone and fascia-bulk soft tissue interactions (3DBPT[1]). To evaluate the effect of fascia-bulk soft tissue interaction on internal foot mechanics, we compared the proposed model with the other two plantar fascia models without fascia-bulk soft tissue interaction. One chose linear plantar fascia, which connected the calcaneal tubercle and every proximal phalange (BPL[2]). The other used a three-dimensional plantar fascia model and only included the fascia-bone interaction (3DBP[3]). In this study, peak foot plantar pressure and plantar fascia stress among the three models will be compared. As the 3DBPT model considered the impact of superoinferior loading caused by the arch support on the plantar fascia, we hypothesized that 3DBPT would produce higher stress in plantar fascia than 3DBP.

2. Methods

In this study, FE models of the foot-ankle complex were developed. The modelling procedures, including participant data collection, geometries reconstruction, materials properties, loading and boundary conditions, and model validation, were described. Moreover, the predicated internal foot biomechanics among three plantar fascia configurations in the foot-ankle complex model were compared, thus evaluating the effects of fascia-bulk soft tissue interaction on the internal foot mechanics.

2.1. Participant information

A young male adult (27 years old, 175 cm height, and 64 kg weight) with flatfoot participated in this study. This study utilized the footprint index [19] and the navicular drop test [20] to identify the foot type. For flatfoot, the footprint index is more than 0.26, and navicular drop is more than 10 mm [19,20]. The arch index and the navicular drop of the subject's right foot are 0.30 and 12 mm, respectively, which was recognized as a flatfoot case. Magnetic resonance imaging (MRI) of the right foot was obtained at 1-mm interval and a resolution of 0.625 mm pixel size with a 3.0-T MRI scanner (Seimens, Erlangen, Germany). The neutral configuration of the ankle joint complex was determined according to the definition of the joint coordinate system proposed by the study [21]. During the MRI scan, a custom ankle-foot orthosis was used to fix the ankle joint in a neutral, unloaded position [22]. Before the experiment, ethical approval was approved by the Human Subjects Ethics Sub-Committee of the Hong Kong Polytechnic University (Number: HSEARS20190124008). The consent form and information form for data collection and research contents were provided and signed before the experiment.

[2] BPL: linear plantar fascia connects calcaneal tubercle and every proximal phalange.

[3] 3DBP: three-dimensional plantar fascia model with fascia-bone interaction.

2.2. Geometry reconstruction

The geometries of the bone and bulk soft tissue of the right foot were obtained using medical image processing software (Mimics 10.1, Materialize Inc., Belgium). The extracted geometries were further processed to obtain solid geometry in Rapidform (INUS Technology Ltd., Seoul, Korea). The foot geometries consisted of the encapsulated bulk tissue and twenty bones, including the distal part of tibia and fibula. The 2 mm thick membrane encapsulated the bulk soft tissue and formed the skin layer. To simplify the model, this model fused the second to fifth interphalangeal joints. For the foot ligaments, 110 bundles of ligaments were modelled as trusses to connect bony structures. These tissues were constructed based on the MRI and confirmed by an orthopedic surgeon. The interior surface of the encapsulated soft tissue was tied to the bony structures. A frictionless contact with a nonlinear contact stiffness was used to define the bones' contact properties [15]. The "hard" contact property was used in the normal direction of bones. The coefficient of friction between the foot surface and ground plate was assumed 0.6 [23]. More information of the FE model can be seen in Fig. 1.

2.3. Plantar fascia model configurations

This study constructed three plantar fascia model configurations, including 3DBPT, 3DBP, and BPL (Fig. 2). In the 3DBPT model, three-dimensional geometry was built for the plantar fascia model. The bulk soft tissue was constructed by subtracting the geometry of plantar fascia. The plantar fascia was tied to the calcaneal tubercle and the proximal phalanges and the inner surface of the bulk soft tissue. In the second model, the three-dimensional geometry of plantar fascia was only attached to the inferior surface of the calcaneal tubercle and the proximal phalanges. The interaction between plantar fascia and bulk soft tissue was ignored. In the third model, linear plantar fascia was used to connect the calcaneal tubercle and every proximal phalange.

2.4. Mesh and materials

This study meshed the foot-ankle complex components in the FE platform Abaqus 6.14 (Simulia, Dassault Systemes, Vélizy-Villacoublay, France). Linear hexahedra element (C3D8) was assigned to the ground plate in this study. Linear tetrahedral element (C3D4) was assigned to the bones and the encapsulated bulk tissue. Three-node triangular membrane element (M3D3) and two-node linear three-dimensional elements (T3D2) were assigned to the skin layer and most of the ligaments, respectively. Moreover, linear tetrahedral elements (C3D4) and two-node linear three-dimensional elements (T3D2) were assigned to the three-dimensional and linear plantar fascia, respectively. All material properties of the model parts were determined from existing literature [24–29]. More specific materials properties of the components were shown in Table 1.

The overall element size was 3 mm for the bone structures, plantar fascia, and 5 mm for the encapsulated soft tissue and ground plate. The elements were refined locally to accommodate small part geometries, contact regions, and abrupt geometrical changes. The mesh convergence test was conducted in a balanced standing condition with a reduction of element size of 10%. The deviations of the peak foot plantar pressure and the peak von Mises stress of the plantar fascia were 4.4% and 3.8%, respectively. The mesh size in the current simulation was believed to be acceptable since the of these parameters' deviations were less than 5% [30].

2.5. Boundary and loading conditions

In this study, the comparison of internal foot forces in three plantar fascia configurations was performed in the balanced standing condition. When standing in balance, body weight is considered to be evenly distributed on both feet. For a subject weighing 64 kg, a vertical upward

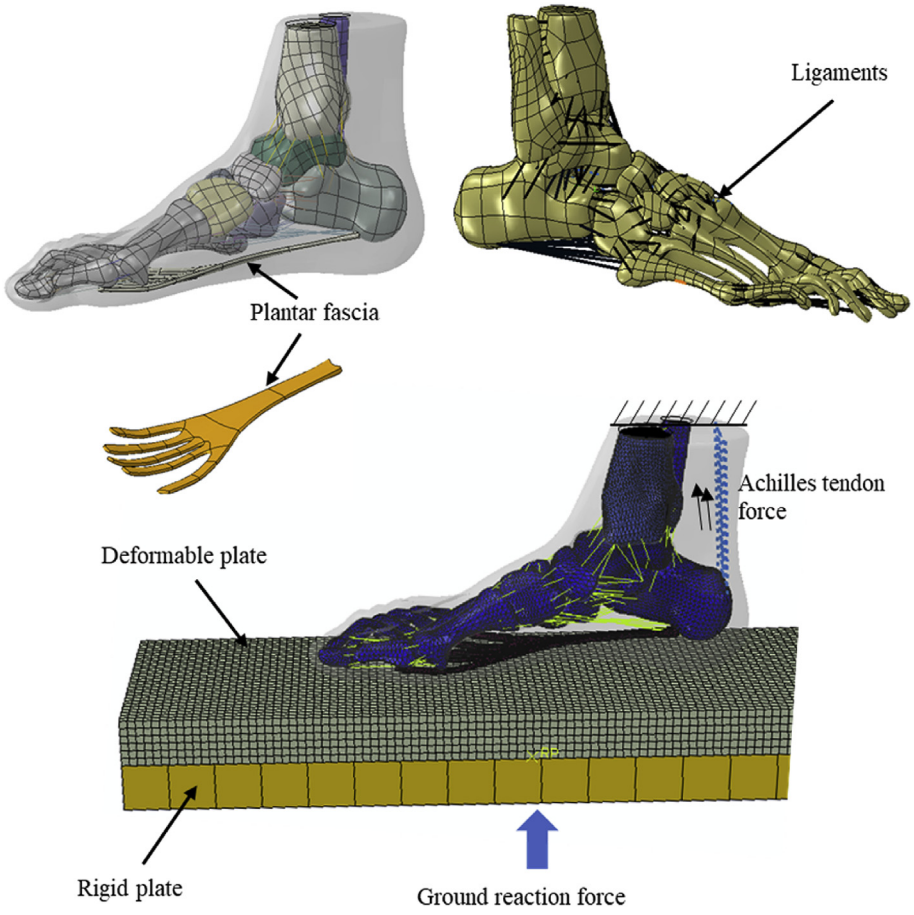

Fig. 1. Overview of the foot-ankle complex finite element model. The bulk soft tissue (transparent) was constructed by subtracting the geometry of plantar fascia and bony structures. And fascia and bones were also tied to the inner surface of the bulk soft tissue. The 2-mm thick membrane encapsulated the bulk soft tissue and formed the skin layer. The bony structures were connected by linear ligaments and plantar fascia. The proximal cross-section surface of the tibia, fibula, and skin was fixed at all degrees of freedom. The triceps surae force was applied to the model via the control unit of the Achilles tendon, modelled as linear connectors. Meanwhile, the ground plate was allowed to move in the vertical direction. One rigid plate was tied to the deformable plate, and the motion and force were applied on the rigid plate.

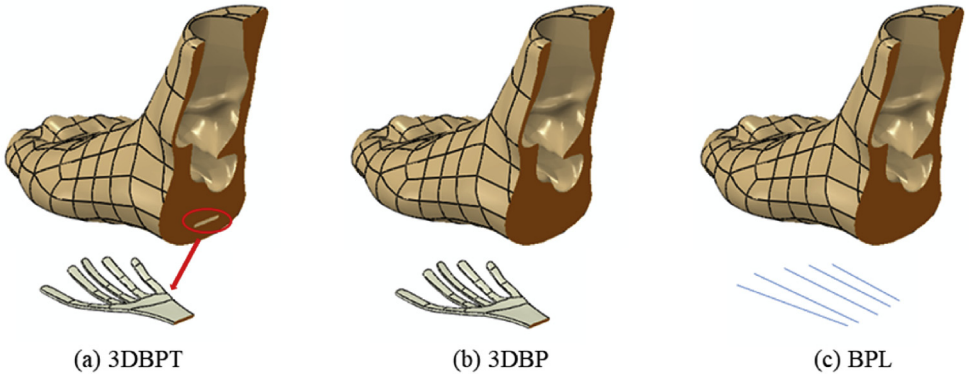

Fig. 2. Comparison of three plantar fascia modelling, (a) 3DBPT: three-dimensional plantar fascia model with both fascia-bone and fascia-bulk soft tissue interactions, (b) 3DBP: three-dimensional plantar fascia model with fascia-bone interaction, (c) BPL: linear plantar fascia connects calcaneal tubercle and every proximal phalange.

force vector of 320 N was applied to the ground in the simulation model. The triceps surae muscle force was applied to the model during the simulation of balanced standing. The magnitude of the triceps surae force, approximately 50% of the ground reaction force, was adopted via the control unit of the Achilles tendon (Simkin, 1982). In this model, the proximal cross-section surfaces of tibia, fibula, and skin were fixed in all degrees of freedom. Meanwhile, the ground plate was allowed to move in the vertical direction. To easily control the motion of ground plate, one rigid plate was tied to the ground plate.

2.6. Model output and analysis

The simulation was conducted with Abaqus 6.14 (Dassault Systèmes, Vélizy-Villacoublay, France) using the standard static solver. The foot plantar contact pressure and von Mises stress on the three-dimensional plantar fascia were reported and compared. Contours of foot contact pressure and stress in the plantar fascia were also plotted. Ten foot ligaments, including bifurcate, calcaneocuboid, calcaneofibular, calcaneonavicular, deltoid, talocalcaneal, cuboideonavicular, talofibular, talonavicular and tibiospring ligaments, were crucial in maintaining the

Table 1
Material properties of the components in the finite element model.

	Elastic modules (MPa)	Poisson ratio	Cross-section (mm^2)	References
Skin	1st-order Ogden hyperelastic model (μ = 0.122 MPa, α=18, Thickness: 2.0 mm)	–		[28]
Bulk soft tissue	second-order polynomial strain hyperelastic model (C_{10}=0.8556, C_{01}=−0.05841, C_{20}=0.03900, C_{11}=−0.02319, C_{02}=0.00851, D_1=3.65273)	–		[26]
Bone	10,000	0.34	–	[27]
Ligaments	260	0.4	18.4	[25]
Three-dimensional Plantar fascia	350	0.45	–	[24]
One-dimensional Plantar fascia	350	0.4	290.7	[29]

foot posture during weight-bearing conditions. The maximum von Mises stresses of these ligaments were reported in the FE model. Meanwhile, the strain distribution of the plantar fascia in the 3DBPT model was reported.

2.7. Model validation

This foot-ankle complex FE model was validated by comparing the foot plantar pressure in the FE model and in vivo measurement under weight-bearing condition. A dynamic foot pressure measurement system (F-scan system, Tekscan, South Boston, MA, United States) was used to record the foot contact pressure of the participant during standing (Fig. 3). The average of 3-s foot pressures during balanced standing was obtained. The foot plantar area was divided into ten parts, including the medial heel, lateral heel, midfoot, first metatarsal, second metatarsal, third metatarsal, fourth metatarsal, fifth metatarsal, hallux, and lesser toes regions, where the maximum contact pressure of each area is extracted for analysis. The correlation analysis was performed on the ten pairs between measurements and predictions to evaluate the agreement for validation. Statistical analysis was conducted with SPSS (Version 19.0, IBM, Armonk, USA) at a significance level of 0.05. The Pearson correlation |r| was categorized as weak, moderate, and strong for $|r| \leq 0.35$, $0.36 \leq |r| \leq 0.67$, $0.68 \leq |r| \leq 1.0$ [31]. Moreover, the predicted plantar strain in the 3DBPT model was validated by comparing the results of an existing study [32]. The tensile strain was measured in the hindfoot region of the plantar fascia in the cadaveric samples [32]. The load-strain curves of plantar fascia were displayed as a polynomial regression curve

Fig. 3. Measurement of foot plantar contact pressure during balancing standing.

of the measured dataset. The calculated plantar fascia strains at the same position were compared with the values in the experiments [32]. In this study, the vertical ground reaction force was 320 N. The strain of the plantar fascia under 320 N could be extracted from the load-strain curves in the experimental study [32].

3. Results

3.1. Validation

The foot plantar pressure distributions and correlation analysis between 3DBPT model prediction and in-vivo measurement were shown in Fig. 4 (A) and 4 (B). The correlation analysis indicated a significant high linear relationship between the measurements and the predictions (r = 0.834 and p = 0.003). Meanwhile, the strain of plantar fascia was predicted during balancing standing (Fig. 5). The percent strain of three samples (1.07 ± 0.21%) under 320 N was obtained from the load-strain curves [32]. The predicted plantar strains of the hindfoot area (red rectangular region) in the 3DBPT model under 320 N ranged from 0.87% to 1.19%, which was within the measurements [32]. These results indicated that our foot-ankle complex model was reasonable.

3.2. Peak foot contact pressures

The foot plantar pressure distributions in three model predictions were compared in Fig. 6. Peak values of the whole foot occurred in the hindfoot area for three model predictions. In the forefoot area, the peak value predicted by 3DBPT (0.13 MPa) was higher than that in 3DBP and BPL (0.123 MPa and 0.099 MPa). As for the hindfoot, the peak value predicted by 3DBPT (0.159 MPa) was lower than that in 3DBP and BPL (0.175 MPa and 0.169 MPa).

3.3. Foot ligaments stresses

The predicted von Mises stresses of foot ligaments in three models were compared in Fig. 7. For the calcaneocuboid, calcaneofibular, calcaneonavicular, deltoid, talonavicular, tibiospring ligaments, the values in the 3DBPT and 3DBP model were larger than those in the BPL model. Moreover, values of cuboideonavicular and talofibular ligaments in 3DBP model were larger than those in the 3DBPT and BPL, while the value of talocalcaneal ligament was lower. As for the bifurcate ligaments, BPL had a higher value than that in 3DBPT and 3DBP models.

3.4. Plantar fascia stress distribution

The plantar fascia stress distribution in 3DBPT and 3DBP were illustrated in Fig. 8. The region that was close to the foot bone was excluded from the contour. The remaining part of the fascia is divided equally into three parts. The stresses in three areas in the 3DBPT model were higher than those in 3DBP (6.25 MPa vs. 4.92 MPa in the distal portion, 4.11 MPa vs. 3.49 MPa in the middle portion, and 7.32 MPa vs. 5.07 MPa in the proximal portion).

4. Discussion

This study has developed a three-dimensional plantar fascia model in the flatfoot FE analysis, which included fascia-bone and fascia-bulk soft tissue interactions. Besides, linear and three-dimensional plantar fascia models without considering the fascia-bulk soft tissue were established. The effects of interaction between fascia-bulk soft tissue on internal foot mechanics were evaluated. Our results supported the hypothesis that the peak stress of plantar fascia increased while considering the interaction between bulk soft tissue and plantar fascia for the three-dimensional plantar fascia model.

The peak foot contact pressure of the 3DBPT model occurred in the hindfoot area, which also showed good agreement with the measured

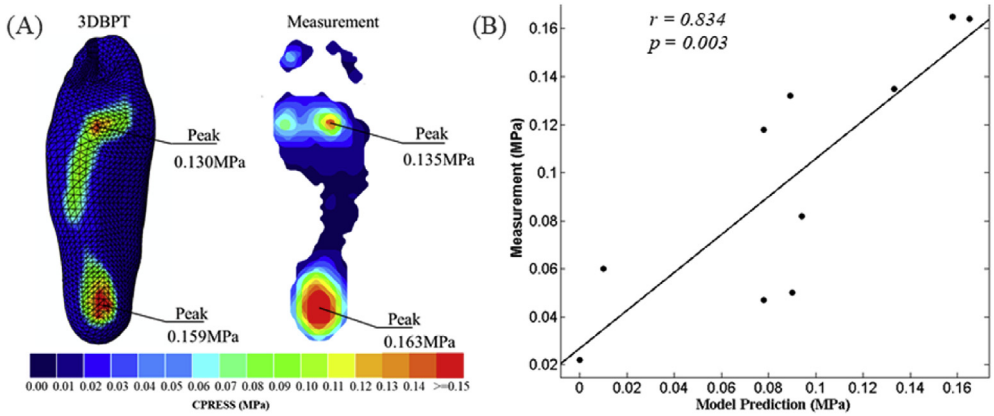

Fig. 4. Validation of the 3DBPT modelling with measurement during balancing standing. (A) Predicted and measured foot pressure distribution, (B) correlation analysis. 3DBPT represents 3D plantar fascia was tied to both bones and bulk soft tissue.

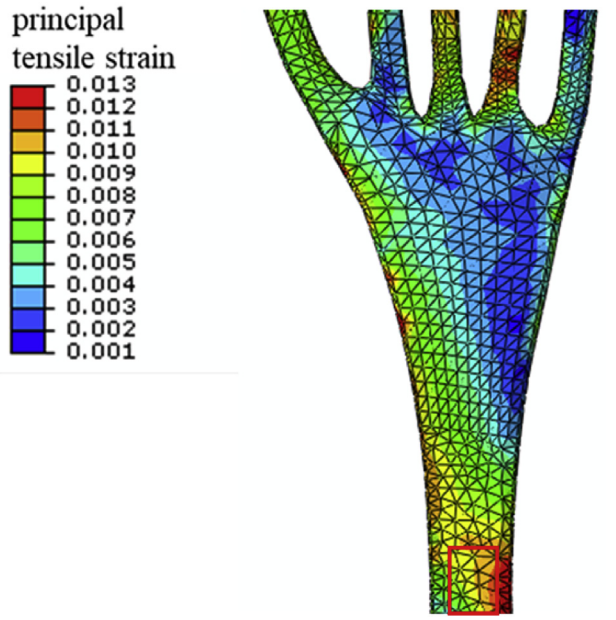

Fig. 5. Strain distribution of plantar fascia in the 3DBPT model. The region that was close to the foot bone was excluded from the contour. 3DBPT represents three-dimensional plantar fascia with both fascia-bone and fascia-bulk soft tissue interactions.

value. Previous studies also indicated that the peak foot contact pressure occurred in the hindfoot area during balanced standing [33,34]. The foot contact pressures in the 3DBPT model and other two models were evaluated and compared. As for the peak pressure in BPL, the percentage error is high in the forefoot area (27%) and low in the hindfoot area (4%). Moreover, the percentage errors for peak pressures of hindfoot and forefoot in the 3DBPT (2–4%) were lower than those in 3DBP (8–9%). The higher accuracy in the 3DBPT model is perhaps due to the more realistic soft tissue connection, in which the plantar fascia was tied to the bulk soft tissue.

For the 3DBPT model, the peak von Mises stress in the proximal region of plantar fascia is higher than those in the middle and distal regions. The results were in line with the previous study, which exhibited stress concentrations at the same locations near the site of heel pain [16]. This study also revealed that the stresses of three fascia areas in the 3DBPT model were higher than those in 3DBP. The 3DBP adopted a similar method with previous studies [7,17], which ignored the interaction between plantar fascia and bulk soft tissue. Through the interaction between bulk soft tissue and plantar fascia in 3DBPT, the force applied to the bulk soft tissue could also be transmitted to the plantar fascia. The increased stress of plantar fascia in 3DBPT may be due to the force applied to the interaction between bulk soft tissue and plantar.

The three-dimensional plantar fascia model, which considered the interaction between plantar fascia and bulk soft tissue, could better represent the physiological constraints of ligamentous structures. In contrast, previous work normally simplified the plantar fascia as linear trusses or spring ligaments [9,15]. One-dimensional ligament could not obtain the internal force distribution and may cause the plantar fascia to be twisted [16]. Three-dimensional geometry of fascia could display the internal force during weight-bearing conditions. Meanwhile, the proposed 3DBPT model that included the interaction between bulk soft tissue and plantar fascia geometry was different from the previous plantar fascia model, which did not include the bulk soft tissue [9,16] or ignored the interaction between bulk soft tissue and plantar fascia [3,7,17]. Ignoring the force transmission between plantar fascia and bulk soft tissue might affect the plantar fascia stress and foot contact pressure.

The peak stresses of the foot ligaments in 3DBPT were compared with 3DBP and BPL models. Overall, the peak values of foot ligaments stress in the linear plantar fascia model showed different patterns compared to the models with three-dimensional plantar fascia. The results indicated that the geometry of plantar fascia modelling altered the biomechanical response of fascia to loading, thus affecting the internal force of soft tissues in the foot. Previous studies also reported that linear trusses could cause the plantar fascia model to be twisted [16]. In 3DBPT and 3DBP models, the peak stress of foot ligaments was similar, except for the calcaneonavicular and talocalcaneal ligaments. However, the influence of interaction between fascia and bulk soft tissue on the foot ligaments could not be ignored. It should be noted that these two models were only compared under balanced standing condition, and the internal force of the foot could alter differently during dynamic walking or insole intervention conditions [35].

Several limitations should be discussed. Firstly, this study modelled the bony and most of the ligamentous structures with materials from previous studies [8,9]. Simplification of the bones and ligaments may influence the internal stress distribution and lead to a decrease in joint stiffness. Secondly, this model only includes triceps surae, while other intrinsic and extrinsic foot muscles were not included. It was reported that triceps surae were the dominant muscles in maintaining the balanced standing, while the influence of other muscles was minimal [36]. Therefore, ignoring other muscles may have little impact on the internal foot force and static equilibrium. Thirdly, FE analysis, particularly on the foot-and-ankle complex, is often confined to single-subject

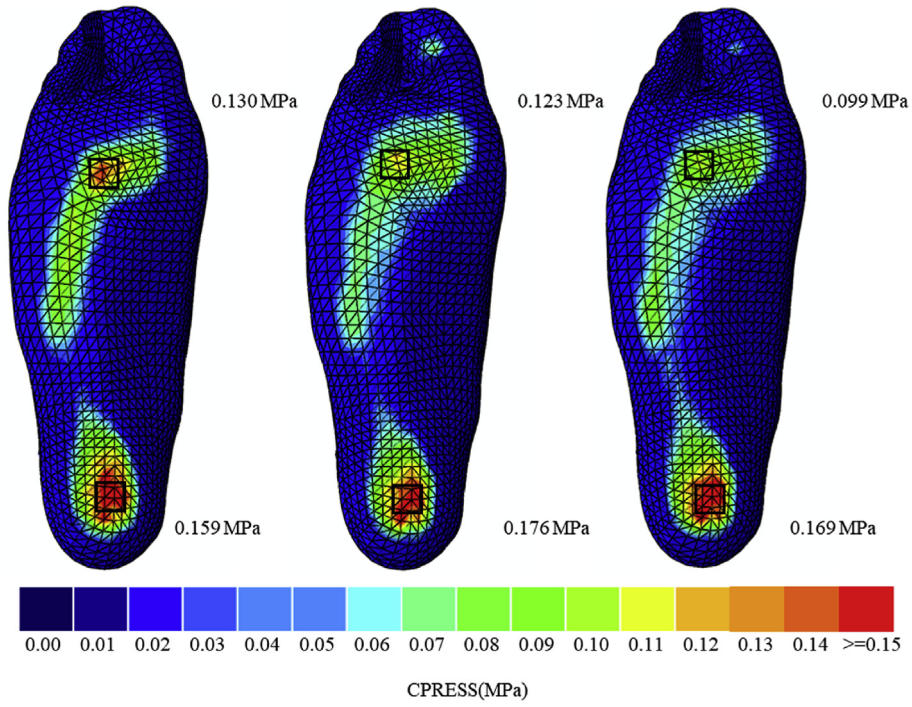

Fig. 6. Comparison of peak foot contact pressure of hindfoot, forefoot, and whole foot in three plantar fascia modelling and measurement during balancing standing. 3DBPT represents three-dimensional plantar fascia with both fascia-bone and fascia-bulk soft tissue interactions, 3DBP represents three-dimensional plantar fascia with fascia-bone interaction, BPL represents linear plantar fascia with fascia-bone interaction. The peak values in forefoot and hindfoot occurred in the black squares.

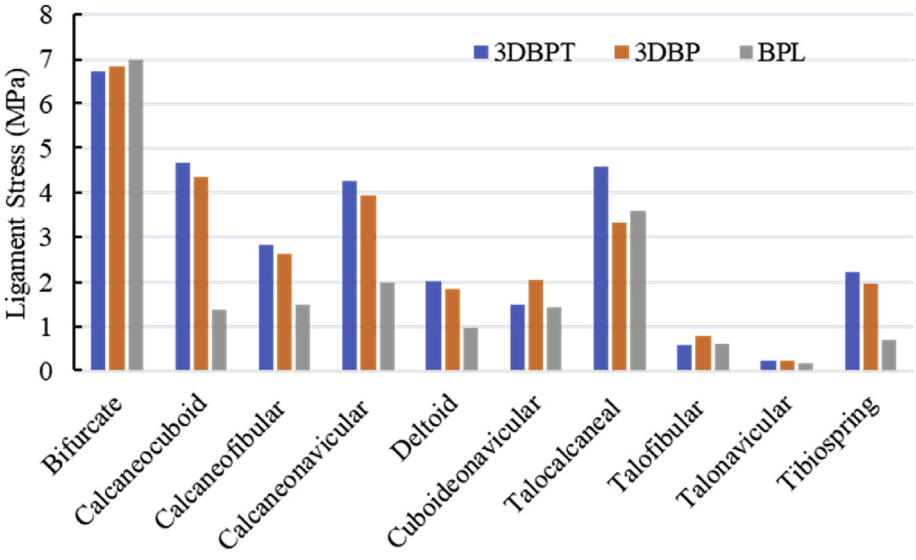

Fig. 7. Comparison of peak von Mises stresses of main ligaments in three plantar fascia modeling during balancing standing, 3DBPT represents three-dimensional plantar fascia with both fascia-bone and fascia-bulk soft tissue interactions, 3DBP represents three-dimensional plantar fascia with fascia-bone interaction, BPL represents linear plantar fascia with fascia-bone interaction.

design which did not account for individual variance, since creating a single model with corresponding validation involves a strenuous amount of work [3,15,37]. This study endeavored to select a typical and representative participant to compromise the external validity issue. Furthermore, validation was performed on the foot contact pressure and plantar fascia strain. More additional in-vivo measurements, such as position alteration of anatomical points in radiographic images during loading conditions, could enhance the reliability of the model [38].

5. Conclusion

This study has developed a flatfoot FE model, which adopted a three-dimensional plantar fascia with both bone-bulk soft tissue and plantar -bulk soft tissue. The proposed model was used to evaluate the influence of fascia-bulk soft tissue interaction on the internal foot mechanics by comparing it with the other two models, which did not include fascia-bulk soft tissue connections. The foot model with three-dimensional plantar fascia could reveal the entire plantar fascia stress distribution.

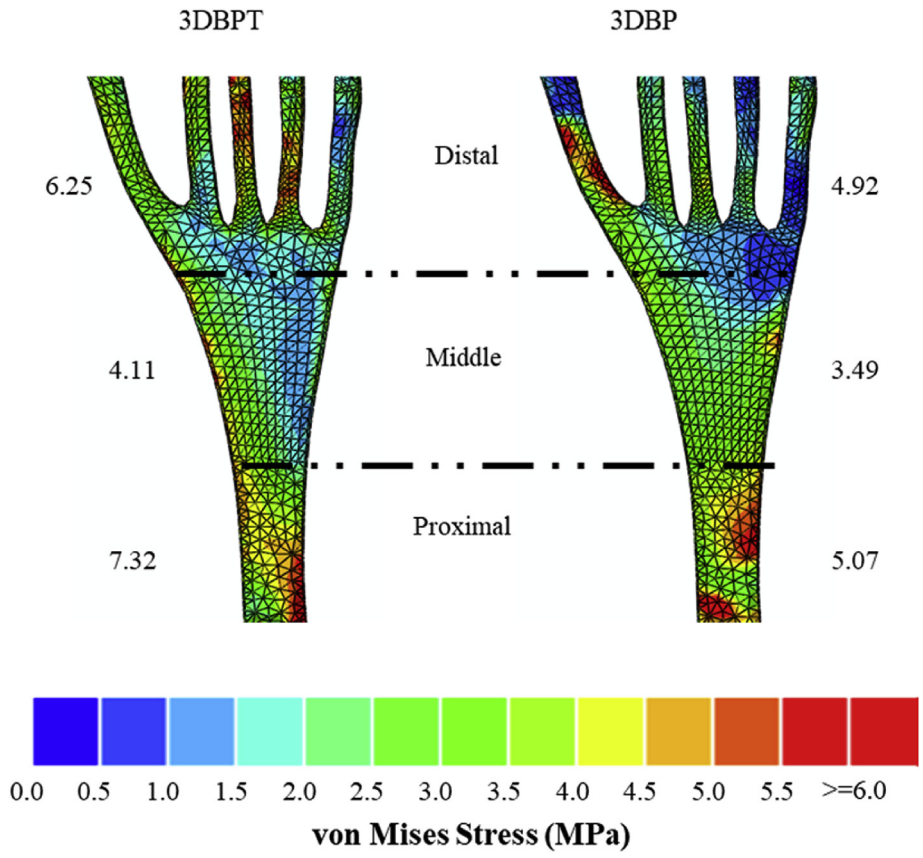

Fig. 8. Comparison of stress distribution of three-dimensional plantar fascia in two models during balancing standing. The plantar fascia was divided into three parts, and the peak values of each part were displayed. 3DBPT represents three-dimensional plantar fascia with both fascia-bone and fascia-bulk soft tissue interactions, 3DBP represents three-dimensional plantar fascia with fascia-bone interaction.

Meanwhile, through the interaction between bulk soft tissue and plantar fascia, the von Mises stresses of the plantar fascia in the 3DBPT model increased by 17.7% – 44.3% compared to the 3DBP model. The proposed model in this study considered the vertical loading for the plantar fascia and could provide a relatively reliable force distribution in fascia during weight-bearing conditions and indicate the deterioration of plantar fascia, thereby contributing to the development of the orthotic designs for flatfoot deformities.

Declaration of competing interest

The authors declare that there are no conflicts of interest.

Acknowledgment

The work was supported by the Key R&D Program granted by the Ministry of Science and Technology of China (number: 2018YFB1107000), the National Natural Science Foundation of China (numbers: 11732015, 11972315), and General Research Fund granted by the Hong Kong Research Grant Council (number: PolyU152065/17E).

References

[1] McDonald KA, Stearne SM, Alderson JA, North I, Pires NJ, Rubenson J. The role of arch compression and metatarsophalangeal joint dynamics in modulating plantar fascia strain in running. PloS One 2016;11(4):e0152602. https://doi.org/10.1371/journal.pone.0152602.

[2] Angin S, Mickle KJ, Nester CJ. Contributions of foot muscles and plantar fascia morphology to foot posture. Gait Posture 2018;61:238–42. https://doi.org/10.1016/j.gaitpost.2018.01.022.

[3] Chen TL-W, Wong DW-C, Peng Y, Zhang M. Prediction on the plantar fascia strain offload upon Fascia taping and Low-Dye taping during running. J Orthop Translat 2020;20:113–21. https://doi.org/10.1016/j.jot.2019.06.006.

[4] Angin S, Crofts G, Mickle KJ, Nester CJ. Ultrasound evaluation of foot muscles and plantar fascia in pes planus. Gait Posture 2014;40(1):48–52. https://doi.org/10.1016/j.gaitpost.2014.02.008.

[5] Irving DB, Cook JL, Menz HB. Factors associated with chronic plantar heel pain: a systematic review. J Sci Med Sport 2006;9(1–2):11–22. https://doi.org/10.1016/j.jsams.2006.02.004. discussion 3-4.

[6] Cheng HY, Lin CL, Chou SW, Wang HW. Nonlinear finite element analysis of the plantar fascia due to the windlass mechanism. Foot Ankle Int 2008;29(8):845–51. https://doi.org/10.3113/FAI.2008.0845.

[7] Guo J, Liu X, Ding X, Wang L, Fan Y. Biomechanical and mechanical behavior of the plantar fascia in macro and micro structures. J Biomech 2018;76:160–6. https://doi.org/10.1016/j.jbiomech.2018.05.032.

[8] Chen TL, Wong DW, Wang Y, Lin J, Zhang M. Foot arch deformation and plantar fascia loading during running with rearfoot strike and forefoot strike: a dynamic finite element analysis. J Biomech 2019;83:260–72. https://doi.org/10.1016/j.jbiomech.2018.12.007.

[9] Cheng HY, Lin CL, Wang HW, Chou SW. Finite element analysis of plantar fascia under stretch-the relative contribution of windlass mechanism and Achilles tendon force. J Biomech 2008;41(9):1937–44. https://doi.org/10.1016/j.jbiomech.2008.03.028.

[10] Wong DW-C, Zhang M, Yu J, Leung AK-L. Biomechanics of first ray hypermobility: an investigation on joint force during walking using finite element analysis. Med Eng Phys 2014;36(11):1388–93. https://doi.org/10.1016/j.medengphy.2014.03.004.

[11] Wang Y, Wong DW-C, Zhang M. Computational models of the foot and ankle for pathomechanics and clinical applications: a review. Ann Biomed Eng 2016;44(1):213–21. https://doi.org/10.1007/s10439-015-1359-7.

[12] Yu J, Wong DW-C, Zhang H, Luo Z-P, Zhang M. The influence of high-heeled shoes on strain and tension force of the anterior talofibular ligament and plantar fascia during balanced standing and walking. Med Eng Phys 2016;38(10):1152–6. https://doi.org/10.1016/j.medengphy.2016.07.009.

[13] Wong DW-C, Wang Y, Chen TL-W, Leung AK-L, Zhang M. Biomechanical consequences of subtalar joint arthroereisis in treating posterior tibial tendon dysfunction: a theoretical analysis using finite element analysis. Comput Methods Biomech Biomed Eng 2017;20(14):1525–32. https://doi.org/10.1080/10255842.2017.1382484.

[14] Hsu YC, Gung YW, Shih SL, Feng CK, Wei SH, Yu CH, et al. Using an optimization approach to design an insole for lowering plantar fascia stress–a finite element study. Ann Biomed Eng 2008;36(8):1345–52. https://doi.org/10.1007/s10439-008-9516-x.

[15] Wong DW-C, Wang Y, Leung AK-L, Yang M, Zhang M. Finite element simulation on posterior tibial tendinopathy: load transfer alteration and implications to the onset of pes planus. Clin Biomech 2018;51:10–6. https://doi.org/10.1016/j.clinbiomech.2017.11.001.
[16] Chen Y-N, Chang CW, Li CT, Chang CH, Lin CF. Finite element analysis of plantar fascia during walking: a quasi-static simulation. Foot Ankle Int 2015;36(1):90–7. https://doi.org/10.1177/1071100714549189.
[17] Akrami M, Qian Z, Zou Z, Howard D, Nester CJ, Ren L. Subject-specific finite element modelling of the human foot complex during walking: sensitivity analysis of material properties, boundary and loading conditions. Biomech Model Mechanobiol 2018;17(2):559–76. https://doi.org/10.1007/s10237-017-0978-3.
[18] Filardi V. Flatfoot and normal foot a comparative analysis of the stress shielding. J Orthop 2018;15(3):820–5. https://doi.org/10.1016/j.jor.2018.08.002.
[19] Roy H, Bhattacharya K, Deb S, Ray K. Rch index: an easier approach for arch height (a regressionanalysis). Al Ameen J Med Sci 2012;5:137–46.
[20] Mueller M, Host J, Norton B. Navicular drop as a composite measure of excessive pronation. J Am Podiatr Med Assoc 1993;83(4):198–202. https://doi.org/10.7547/87507315-83-4-198.
[21] Wu G, Siegler S, Allard P, Kirtley C, Leardini A, Rosenbaum D, et al. ISB recommendation on definitions of joint coordinate system of various joints for the reporting of human joint motion—part I: ankle, hip, and spine. J Biomech 2002;35(4):543–8. https://doi.org/10.1016/S0021-9290(01)00222-6.
[22] Yu J. Development of a computational foot model for biomechanical evaluation of high-heeled shoe designs. The Hong Kong Polytechnic University; 2009.
[23] Zhang M, Mak AF. In vivo friction properties of human skin. Prosthet Orthot Int 1999;23(2):135–41. https://doi.org/10.3109/03093649909071625.
[24] Wright DG, Rennels DC. A study of the elastic properties of plantar fascia. JBJS 1964;46(3).
[25] Siegler S, Block J, Schneck CD. The mechanical characteristics of the collateral ligaments of the human ankle joint. Foot Ankle 1988;8(5):234–42. https://doi.org/10.1177/107110078800800502.
[26] Lemmon D, Shiang TY, Hashmi A, Ulbrecht JS, Cavanagh PR. The effect of insoles in therapeutic footwear—a finite element approach. J Biomech 1997;30(6):615–20. https://doi.org/10.1016/S0021-9290(97)00006-7.
[27] Chen W-P, Ju C-W, Tang F-T. Effects of total contact insoles on the plantar stress redistribution: a finite element analysis. Clin Biomech 2003;18(6):S17–24. https://doi.org/10.1016/S0268-0033(03)00080-9.
[28] Pailler-Mattei C, Bec S, Zahouani H. In vivo measurements of the elastic mechanical properties of human skin by indentation tests. Med Eng Phys 2008;30(5):599–606. https://doi.org/10.1016/j.medengphy.2007.06.011.
[29] Chen W-M, Lee T, Lee PV-S, Lee JW, Lee S-J. Effects of internal stress concentrations in plantar soft-tissue—a preliminary three-dimensional finite element analysis. Med Eng Phys 2010;32(4):324–31. https://doi.org/10.1016/j.medengphy.2010.01.001.
[30] Henninger HB, Reese SP, Anderson AE, Weiss JA. Validation of computational models in biomechanics. Proc Inst Mech Eng H 2010;224(7):801–12. https://doi.org/10.1243/09544119JEIM649.
[31] Taylor R. Interpretation of the correlation coefficient: a basic review. J Diagn Med Sonogr 1990;6(1):35–9. https://doi.org/10.1177/875647939000600106.
[32] Kogler GF, Solomonidis SE, Paul JP. In vitro method for quantifying the effectiveness of the longitudinal arch support mechanism of a foot orthosis. Clin Biomech 1995;10(5):245–52. https://doi.org/10.1016/S0021-9290(97)00006-7.
[33] Cheung JT, Zhang M, Leung AK, Fan YB. Three-dimensional finite element analysis of the foot during standing–a material sensitivity study. J Biomech 2005;38(5):1045–54. https://doi.org/10.1016/j.jbiomech.2004.05.035.
[34] Su S, Mo Z, Guo J, Fan Y. The effect of arch height and material hardness of personalized insole on correction and tissues of flatfoot. J Healthc Eng 2017;2017:8614341. https://doi.org/10.1155/2017/8614341.
[35] Peng Y, Wong DW, Wang Y, Chen TL, Tan Q, Chen Z, et al. Immediate effects of medially posted insoles on lower limb joint contact forces in adult acquired flatfoot: a pilot study. Int J Environ Res Publ Health 2020;17(7):2226. https://doi.org/10.3390/ijerph17072226.
[36] Basmajian JV, Stecko G. The role OF muscles IN arch support OF the foot. J Bone Joint Surg Am 1963;45:1184–90.
[37] Wong DW-C, Wang Y, Chen TL-W, Yan F, Peng Y, Tan Q, et al. Finite element analysis of generalized ligament laxity on the deterioration of hallux valgus deformity (bunion). Front Bioeng Biotechnol 2020;8:1062. https://doi.org/10.3389/fbioe.2020.571192.
[38] Cifuentes-De la Portilla C, Larrainzar-Garijo R, Bayod J. Analysis of the main passive soft tissues associated with adult acquired flatfoot deformity development: a computational modeling approach. J Biomech 2019;84:183–90. https://doi.org/10.1016/j.jbiomech.2018.12.047.